Journal of Sound and Vibration (1997) **206**(5), 725–735

ON THE BEHAVIOR OF MATERIAL DAMPING DUE TO MULTI-FREQUENCY EXCITATION

H. L. WETTERGREN

Department of Mechanical Engineering, Linköping University, 58183 *Linköping, Sweden*

(*Received* 5 *September* 1996, *and in final form* 9 *June* 1997)

The paper is concerned with the dissipative behavior due to multi-frequency excitation. It is shown both theoretically and experimentally that it is possible to treat the frequencies separately. Practically, this leads for instance to the conclusion that the material damping in a rotor with anisotropic bearings can be treated as a complex stiffness, which simplifies the calculations dramatically.

1. INTRODUCTION

Material damping gives energy dissipation due to internal damping of material. It is assumed that the energy dissipation per cycle is independent of frequency and is proportional to the square of the amplitude. This type of damping is normally called linear or quadratic and leads to an elliptical σ–ε loop. The hysteresis loop corresponding to such behaviour is shown in Figure 1 for three different strain amplitudes. (A list of nomenclature is given in the Appendix.)

Most materials have non-quadratic damping with cyclic energy dissipation proportional to the amplitude of deflection powered by a value between two and three [1]. However, the linear damping (the deflection squared) is convenient to use since it leads to it being possible to use an equivalent viscous damping constant,

$$c_{eq} = h_i / |\omega|, \tag{1}$$

where c_{eq} is the equivalent viscous damping constant, h_i is the hysteretic material damping constant and ω is the vibrational frequency. Problems arise when the mechanical system is excited at more than one frequency. The above substitution is then no longer valid. The present paper deals with this problem. An assumption is made, and confirmed both theoretically and experimentally. Finally, an application is given which shows the advantage of the suggested assumption.

2. THEORETICAL MODEL

The most suitable way of handling rate-independent dissipation that leads to pointed hysteretic loops is some kind of constitutive equation. One constitutive equation is the Davidenkov expression [2]. This expression has been used by others to solve several classes of non-linear problems. Davidenkov used the following slopes of the σ–ε loop,

$$\uparrow \mathrm{d}\sigma/\mathrm{d}\varepsilon = E_t\,[1 - f_1(\varepsilon)], \qquad \downarrow \mathrm{d}\sigma/\mathrm{d}\varepsilon = E_t\,[1 + f_2(\varepsilon)], \tag{2, 3}$$

0022–460X/97/400725 + 11 $25.00/0/sv971149

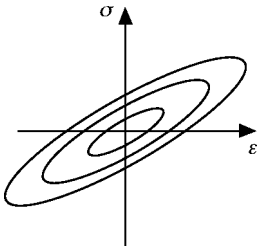

Figure 1. Linear hysteretic material damping.

with the constraints

$$\uparrow\sigma_{\varepsilon=\varepsilon_a} = \downarrow\sigma_{\varepsilon=\varepsilon_a} = -\uparrow\sigma_{\varepsilon=-\varepsilon_a} = -\downarrow\sigma_{\varepsilon=-\varepsilon_a}. \tag{4}$$

Davidenkov chose some particular functions of strain and finally arrived at the following constitutive equations

$$\uparrow\sigma(\varepsilon) = E_t\,[\varepsilon - (H/r)\{(\varepsilon_a + \varepsilon)^r - 2^{r-1}\varepsilon_a^r\}], \tag{5}$$

$$\downarrow\sigma(\varepsilon) = E_t\,[\varepsilon + (H/r)\{(\varepsilon_a - \varepsilon)^r - 2^{r-1}\varepsilon_a^r\}], \tag{6}$$

where H and r are material parameters which have to be determined.

The virgin function or the initial tension curve can be determined by using Masing's rule [3]. For the normalized curve in Figure 2, the parametric virgin function is

$$\sigma(\varepsilon/\varepsilon_a) = \tfrac{1}{2}\left\{\uparrow\sigma\left(2\,\frac{\varepsilon}{\varepsilon_a} - 1\right) + \sigma_a\right\}. \tag{7}$$

Equations (5) and (6) give the stresses when the loading behavior is periodic. If the loading function is an arbitrary function, then it is more convenient to use a discrete material model. A parallel-series model given by Iwan [4] (see Figure 3) has proved to give fair accuracy and to be effective. By using the same principle as Iwan, the loading behavior may be described as

$$\sigma = \sum_{i=1}^{n} E_i\,\varepsilon + \sum_{i=n+1}^{N} \sigma_{f,i}, \tag{8}$$

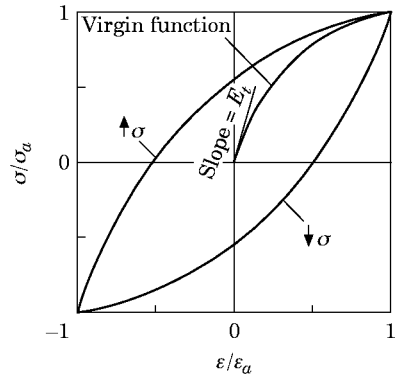

Figure 2. Stress–strain relations according to the Davidenkov equations.

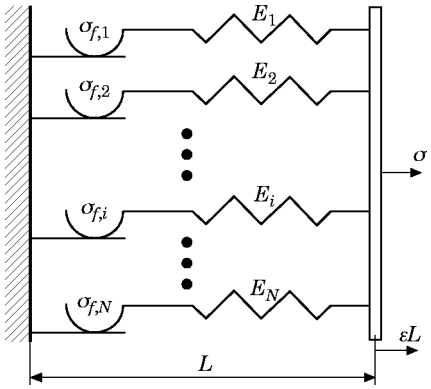

Figure 3. The parallel–series model.

where the summation from 1 to n includes all of those elements that remain elastic after loading to a displacement εL and the summation from $n+1$ to N includes all those "elements" that have "slipped". The elasticity E_i and the "friction" stress $\sigma_{f,i}$ can be determined from the "virgin" force–displacement function in equation (2).

The parallel-series model accordingly consists of a number of elastic springs and slip elements, as shown in Figure 3.

The virgin function may now, with the use of the parallel-series model, be used in reversed order to determine the σ–ε loop for a material subjected to multi-frequency excitation given by

$$\varepsilon = \varepsilon_1 \sin(\omega t) + \varepsilon_{n_{sup}} \sin(n_{sup}\,\omega t), \tag{9}$$

where n_{sup} is a positive integer. An example of equation (9) is shown in Figure 4, where n_{sup} is equal to ten.

For a harmonic loop, the damping energy can be obtained by integrating equations (5) and (6). In terms of the hysteretic loop parameters, the damping energy becomes

$$\Delta U = \frac{2^{r+1}(r-1)HE_t}{r(r+1)}\,\varepsilon_a^{r+1}. \tag{10}$$

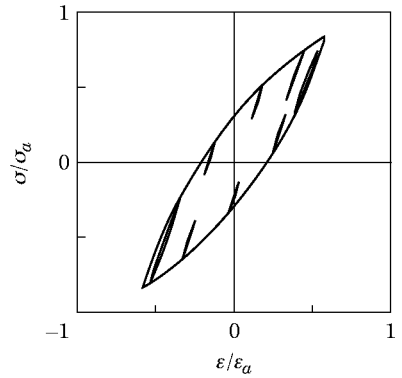

Figure 4. Stress-strain relations due to multi-frequency excitation.

From equation (10), the loss coefficient can be expressed as

$$\eta = \frac{2^{r+1}(r-1)H}{\pi r(r+1)}\,\varepsilon_a^{r-1}. \tag{11}$$

As was mentioned earlier, most materials have a non-quadratic damping proportional to a value between two and three. This is also the case for most constitutive equations. Equation (10) is valid only if r is larger than one. If r is equal to one the loss coefficient in equation (11) is equal to zero! The aim of this study is to find out how to deal with material damping in a rotor.

The material in a rotating shaft may be subjected to several frequencies at the same time. Can these frequencies be treated separately, or in other words: is the dissipated energy for the motion equal to the sum of the main motion and all the sub-motions? If the answer to this question is yes, the method presented in section 4 is valid.

To simplify the writing, let $\sigma_a = \varepsilon_a = 1$ and assume, for instance,

$$\varepsilon = 0{\cdot}5 \sin(\omega t) + 0{\cdot}1 \sin(n_{sup}\,\omega t). \tag{12}$$

The energy dissipation per cycle is

$$\Delta U = \oint \sigma(0{\cdot}5 \sin(\omega t) + 0{\cdot}1 \sin(n_{sup}\,\omega t))\,\mathrm{d}\varepsilon. \tag{13}$$

If the two frequencies are treated separately the dissipated energy for the motion, equal to the sum of those of the main motion and all the sub-motions, becomes

$$\Delta U = \oint \sigma(0{\cdot}5 \sin \omega t)\,\mathrm{d}\varepsilon + n_{sup} \oint \sigma(0{\cdot}1 \sin \omega t)\,\mathrm{d}\varepsilon. \tag{14}$$

Let the loss coefficient in equation (11) be equal to 0·01 and let r in equation (11) be equal to 1·01, meaning that the loss coefficient is in principle independent of the strain amplitude; recall that $\sigma_a = \varepsilon_a = 1$. Equations (13) and (14) for this case are shown in Figure 5. The agreement is good.

The same analysis has been done for other ratios of amplitudes and the results are similar to that in Figure 5. It seems to be a fair assumption to treat the two frequencies separately.

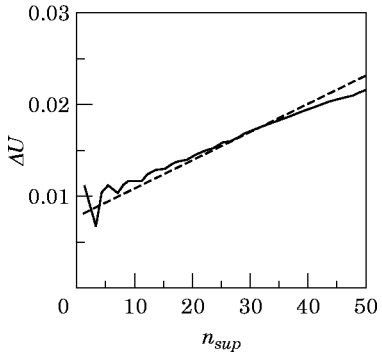

Figure 5. Energy dissipation for different multi-frequency excitation. ——, Equation (13); – – – –, equation (14).

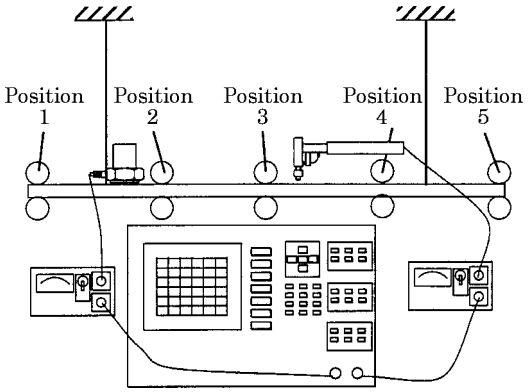

Figure 6. The experimental set-up.

3. EXPERIMENTAL INVESTIGATION

The experimental apparatus used is shown in Figure 6. The components included are a HP 35660A Dynamic Signal Analyzer, impact hammer, accelerometer, test specimen and two rubber bands. The test specimen was a flat laminate that was suspended horizontally in two weak rubber bands, simulating a free–free beam. The specimen width was nominally 55 mm. The specimen was made from carbon/epoxy unidirectional prepreg tape with a total thickness of 3·2 mm.

Four measurements were made: the first (1) without any additional masses on the specimen; and the second (2) and third (3) with one mass at each end and one mass in the middle. In measurement number 2 the weight was 32 g for each mass and in number 3 it was 388 g. Finally, one measurement (4) was made with one 388 g mass at each end and one 388 g mass 0·3 m from each end. The masses are chosen so that experiments 3 and 4 have the same first eigenfrequency, and that the first eigenfrequency of experiment 2 is in agreement with the second eigenfrequency of experiment 4; see Table 1. The weight of the composite specimen was 284 g. The beam was excited with the impact hammer. The eigenfrequencies and mode damping for the lowest two frequencies were measured in the same experiment. The results are shown in Table 2.

The object of this experiment was to see if the first mode damping is the same for experiemts 3 and 4, and that the first mode damping of experiment 2 is in agreement with the second mode damping of experiment 4. It is specially important to notice that the first mode damping of experiment 2 (1·76%) and the second mode damping of experiment 4 (1·50%) are almost the same, which is not obvious in advance. As the damping is the most difficult of the modal parameters to determine, the results seem to confirm the assumption

TABLE 1

Weights of the applied masses

	Position 1 and 5	Position 2 and 4	Position 3
Experiment	weight (g)		
1	—	—	—
2	32	—	32
3	388	—	388
4	388	388	—

TABLE 2

Eigenfrequencies and damping for the specimen

	Eigenmode 1		Eigenmode 2	
Experiment	f_{e1} (Hz)	η (%)	f_{e2} (Hz)	η (%)
1	14·8	1·5	41·8	1·9
2	9·3	1·76	33·0	1·47
3	3·6	1·56	23·8	1·49
4	3·6	1·52	9·3	1·50

that the damping of each mode can be treated separately. In fact the damping for mode 1 in all four experiments seems to be almost the same as the damping of mode 2.

The experimental investigation seems to emphasize the conclusion from the theoretical investigation: namely, that for a multi-frequency excited system with material damping it seems to be a fair assumption to treat the two frequencies separately.

4. APPLICATION

In Figure 7 the disc of mass m carried by a flexible shaft with stiffness k_i and damping c_i is mounted on two rigid supports. The rotor rotates with the angular velocity Ω. A rotating excitation force, F, acts on the disc.

Let the x–y–z co-ordinate system be fixed in space and the ξ–η–z co-ordinate system be fixed in the shaft (rotating with angular velocity Ω). The transformation of the co-ordinates between these two systems is

$$\begin{Bmatrix} \xi \\ \eta \end{Bmatrix} = \begin{bmatrix} \cos \Omega t & \sin \Omega t \\ -\sin \Omega t & \cos \Omega t \end{bmatrix} \begin{Bmatrix} x \\ y \end{Bmatrix}, \tag{15}$$

and the transformation of the forces is

$$\begin{Bmatrix} F_x \\ F_y \end{Bmatrix} = \begin{bmatrix} \cos \Omega t & -\sin \Omega t \\ \sin \Omega t & \cos \Omega t \end{bmatrix} \begin{Bmatrix} F_\xi \\ F_\eta \end{Bmatrix}. \tag{16}$$

If the damping is viscous, then the internal forces acting on the mass are

$$F_\xi = -k_i \xi - c_i \dot{d\xi}, \qquad F_\eta = -k_i \eta - c_i \dot{\eta}, \tag{17}$$

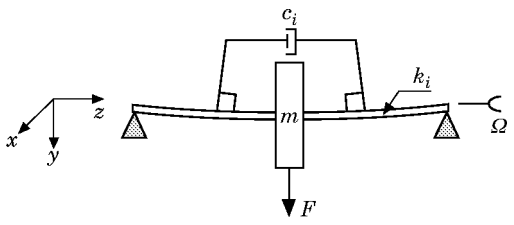

Figure 7. A schematic figure of a rotor with internal damping.

where c_i is the viscous internal damping constant. Equation (15) gives

$$\dot{\xi} = \dot{x}\cos\Omega t + \dot{y}\sin\Omega t + \Omega(-x\sin\Omega t + y\cos\Omega t),$$
$$\dot{\eta} = -\dot{x}\sin\Omega t + \dot{y}\cos\Omega t + \Omega(-x\cos\Omega t - y\sin\Omega t). \tag{18}$$

Equation (16) with equations (17) and (18) give the forces transformed to the global system as

$$\begin{aligned} F_x = &-k_i\,(x\cos\Omega t + y\sin\Omega t)\cos\Omega \\ &- c_i\,(\dot{x}\cos\Omega t + \dot{y}\sin\Omega t + \Omega(-x\sin\Omega t + y\cos\Omega t))\cos\Omega t \\ &+ k_i\,(-x\sin\Omega t + y\cos\Omega t)\sin\Omega t \\ &+ c_i\,(-\dot{x}\sin\Omega t + \dot{y}\cos\Omega t + \Omega(-x\cos\Omega t - y\sin\Omega t))\sin\Omega t. \end{aligned} \tag{19}$$

and in the same manner in the y-direction. Using

$$\sin^2\Omega t + \cos^2\Omega t = 1 \tag{20}$$

gives

$$F_x = -k_i\,x - c_i\,\dot{x} - c_i\,\Omega y, \qquad F_y = -k_i\,y - c_i\,\dot{y} + c_i\,\Omega x. \tag{21}$$

The equations of motion for the system in Figure 7 become

$$m\ddot{x} + c_i\,\dot{x} + k_i\,x + c_i\,\Omega y = F\cos\omega t,$$
$$m\ddot{y} + c_i\,\dot{y} + k_i\,y - c_i\,\Omega x = F\sin\omega t, \tag{22}$$

By using complex notation equations (22) can be written as

$$\begin{bmatrix} k_i - m\omega^2 + \mathrm{i}c_i\,\omega & c_i\,\Omega \\ -c_i\,\Omega & k_i - m\omega^2 + \mathrm{i}c_i\,\omega \end{bmatrix}\begin{Bmatrix} x \\ y \end{Bmatrix} = \begin{Bmatrix} F \\ -\mathrm{i}F \end{Bmatrix}\mathrm{e}^{i\omega t}, \tag{23}$$

where x and y are complex displacements. If the internal damping is hysteretic it is possible to replace c_i by $h_i/|\omega - \Omega|$. The response for the rotor in Figure 7 is now obtained by solving the system

$$\begin{bmatrix} a_{11} & a_{12} \\ a_{21} & a_{22} \end{bmatrix}\begin{Bmatrix} x \\ y \end{Bmatrix} = \begin{Bmatrix} F \\ -\mathrm{i}F \end{Bmatrix}\mathrm{e}^{i\omega t}, \tag{24}$$

where

$$a_{11} = a_{22} = (k_i - m\omega^2) + \mathrm{i}\omega h_i/|\omega - \Omega|,$$
$$a_{12} = -a_{21} = \Omega h_i/|\omega - \Omega|. \tag{25}$$

When the orbit of the motion is circular it can, for instance, be written as

$$x = x_0\cos(\omega t), \qquad y = x_0\cos(\omega t - \pi/2), \tag{26}$$

or, in complex notation $y = -\mathrm{i}x$. Equation (22) can then be rewritten, which leads to

$$a_{11} = a_{22} = (k_i - m\omega^2) + \mathrm{i}h_i \operatorname{sign}(\omega - \Omega), \qquad a_{12} = a_{21} = 0. \tag{27}$$

In equations (27) it can be seen that if the motion is circular the hysteretic damping can be treated as a complex stiffness. If the motion is not circular, however, the trick of replacing c_i by $h_i / |\omega - \Omega|$ will not lead to a frequency independent damping. An elliptical motion, for instance, is obtained when bearings have different stiffnesses in different directions.

The elliptical motion of the rotor may be described in a rotating co-ordinate system. The elliptical motion will be divided into two parts with two different frequencies.

In the fixed co-ordinate system the motion of the rotor is an ellipse described as

$$x = x_0 \cos(\omega t - a_x), \qquad y = y_0 \sin(\omega t - a_y), \tag{28}$$

where ω is a vibration frequency, and a_x and a_y are the phase angles.

Elliptical motion is possible if the rotor bearings are elastically supported on springs of different stiffness, k_{xx} and k_{yy}, in the x and y directions. Let the shaft deflections at the bearings be x_e and y_e. If the phase angle is omitted, equation (15) gives the deflection of the shaft in the rotating system, as

$$\xi = \frac{(x_0 - x_{e0}) + (y_0 - y_{e0})}{2} \cos((\omega - \Omega)t) + \frac{(x_0 - x_{e0}) - (y_0 - y_{e0})}{2} \cos((\omega + \Omega)t),$$

$$\eta = \frac{(x_0 - x_{e0}) + (y_0 - y_{e0})}{2} \sin((\omega - \Omega)t) - \frac{(x_0 - x_{e0}) - (y_0 - y_{e0})}{2} \sin((\omega + \Omega)t). \tag{29}$$

The motion in equations (29) gives the forces from the viscous internal damping on the shaft as

$$F_\xi = -\frac{x_0 - x_{e0} + y_0 - y_{e0}}{2} (\omega - \Omega) c_{(\omega - \Omega)} (\sin((\omega - \Omega)t))$$

$$- \frac{(x_0 - x_{e0}) - (y_0 - y_{e0})}{2} (\omega + \Omega) c_{(\omega + \Omega)} (\sin((\omega + \Omega)t)). \tag{30}$$

$$F_\eta = \frac{x_0 - x_{e0} + y_0 - y_{e0}}{2} (\omega - \Omega) c_{(\omega - \Omega)} (\cos((\omega - \Omega)t))$$

$$- \frac{(x_0 - x_{e0}) - (y_0 - y_{e0})}{2} (\omega + \Omega) c_{(\omega + \Omega)} (\cos((\omega + \Omega)t)). \tag{31}$$

where $c_{(\omega - \Omega)}$ and $c_{(\omega + \Omega)}$ are viscous internal damping constants. Equation (16) gives the forces in equations (30) and (31) in the fixed co-ordinate system.

The forces in equations (30) and (31) give the response for the rotor in Figure 7. Upon introducing the bearing stiffnesses k_{xx} and k_{yy} in the x- and y-directions (see Figure 8), the new response is consequently obtained by solving the system of equations

$$\begin{bmatrix} a_{11} & a_{12} & a_{13} & a_{14} \\ a_{21} & a_{22} & a_{23} & a_{24} \\ a_{31} & a_{32} & a_{33} & a_{34} \\ a_{41} & a_{42} & a_{43} & a_{44} \end{bmatrix} \begin{Bmatrix} x \\ x_e \\ y \\ y_e \end{Bmatrix} = \begin{Bmatrix} F \cos \omega t \\ 0 \\ \mathrm{F} \sin \omega t \\ 0 \end{Bmatrix}, \tag{32}$$

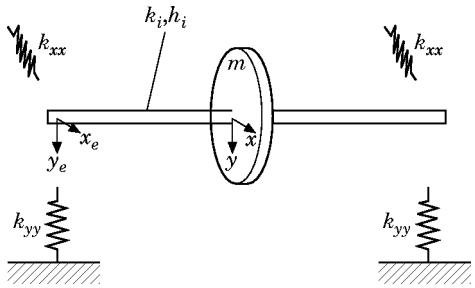

Figure 8. A simple rotor with a symmetric shaft and anisotropic bearings.

where, for instance, a_{11} becomes

$$a_{11} = (k_i - m\omega^2)\cos\omega t + \frac{(c_{(\omega-\Omega)} - c_{(\omega+\Omega)})}{2}\Omega\sin\omega t - \frac{(c_{(\omega-\Omega)} + c_{(\omega+\Omega)})}{2}\Omega\sin\omega t, \quad (33)$$

and similarly for the rest of the terms. If the internal damping is viscous and the motion is circular the damping coefficients are by definition given by

$$c_{(\omega-\Omega)} = c_{(\omega+\Omega)} = c_i. \quad (34)$$

In contrast to a circular motion, the same kind of equivalence as in equation (27) is *not* obtained by replacing c_i by $h_i/|\omega - \Omega|$. However, by using the substitutions

$$c_{(\omega-\Omega)} = h_i/|\omega - \Omega|, \qquad c_{(\omega+\Omega)} = h_i/|\omega + \Omega|, \quad (35)$$

and rewriting in complex form then if $\omega > \Omega$ the non-zero terms in the symmetric matrix become, after some simplifications,

$$a_{11} = a_{33} = (k_i - m\omega^2) + \mathrm{i}h_i, \qquad a_{22} = (k_i + 2k_{xx} - m\omega^2) + \mathrm{i}h_i$$
$$a_{44} = (k_i + 2k_{yy} - m\omega^2) + \mathrm{i}h_i, \qquad a_{12} = a_{34} = -(k_i + \mathrm{i}h_i) \quad (36)$$

where h_i is the internal damping. In equations (36) it can be seen that the hysteretic damping can be treated as a complex stiffness even though the motion is elliptical. However, if $\Omega > \omega$, equation (32) becomes

$$\begin{bmatrix} k_i - m\omega^2 & -k_i & h_i & -h_i \\ -k_i & 2k_{xx} + k_i - m\omega^2 & -h_i & h_i \\ -h_i & h_i & k_i - m\omega^2 & -k_i \\ h_i & -h_i & -k_i & 2k_{yy} + k_i - m\omega^2 \end{bmatrix} \begin{Bmatrix} x_0 \\ x_{e0} \\ y_0 \\ y_{e0} \end{Bmatrix} = \begin{Bmatrix} F\cos\omega t \\ 0 \\ F\sin\omega t \\ 0 \end{Bmatrix}. \quad (37)$$

An explanation for the difference in these two equations can be seen in Figure 9. The elliptical motion given by equation (28) is divided up into one forward and one backward motion. When $\Omega > \omega$ the direction of the damping force of the largest circular motion is changed. The summations of the forward and backward damping forces will then be different.

For those cases in which material damping may have to be considered, the bearings have to be much stiffer than the shaft. The response will then be due to an applied harmonic force, such as the unbalance load, which is often a circle. In such a case, and the excitation frequency is not close to an eigenfrequency the vibration amplitudes of the shaft, $x_0 - x_{e0}$

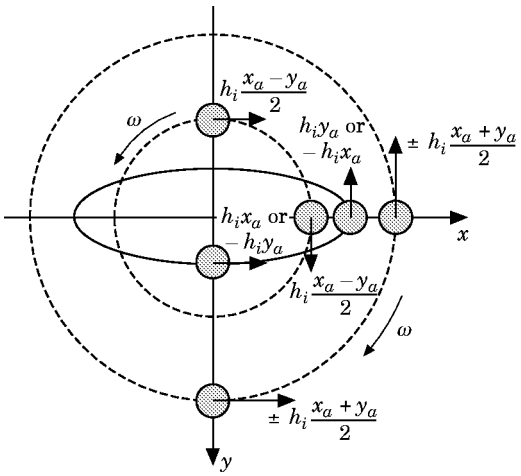

Figure 9. Elliptical motion divided up into forward and backward circular motions.

and $y_0 - y_{e0}$, will be close to each other. Equation (36) may than be used but the internal damping, h_i, has to be treated as negative when $\Omega > \omega$. However, in instability analyses the circular assumption is normally not valid.

Introduce the ellipticity constant, Δ, defined as

$$\Delta = \{(x_0 - x_{e0}) - (y_0 - y_{e0})\}/\{(x_0 - x_{e0}) + (y_0 - y_{e0})\}, \tag{38}$$

where $x_0, \ldots$ is defined in equation (28). By integrating the damping forces round an elliptical orbit it can then be shown that the ratio between the complex, $\Delta E_{complex}$, and exact, ΔE_{exact}, dissipated energy is

$$\Delta E_{complex}/\Delta E_{exact} = (1 + \Delta^2)/(1 - \Delta^2). \tag{39}$$

When the eccentricity is high the vibrational motion will be an ellipse with high Δ.

It may be pointed out that by using the complex stiffness the damping will be treated exactly for subcritical rotational speeds and conservatively for supercritical speeds.

5. CONCLUSIONS

The traditional equivalent damping constant $c_{eq} = h_i/|\omega|$ is valid only when the motion is circular. When the material is subjected to cyclic forces with more than one frequency this substitution is no longer valid. It is, however, shown both theoretically and experimentally in this paper that if the material damping is close to linear it is possible to treat the frequencies separately. An example is given for a rotor with internal material damping supported in anisotropic bearings. The results show that if the ellipticity is small it is, even for a rotor with this kind of bearings, possible to treat the material damping as a complex stiffness.

REFERENCES

1. B. J. Lazan 1968 *Damping of Materials and Members in Structural Mechanics*. Oxford: Pergamon Press.
2. D. Davidenkov 1938 *Journal of Technical Physics* **8**, 483–499. Energy dissipation in vibrations.

3. J. LEMAITRE and J.-L. CHABOCHE 1990 *Mechanics of Solid Materials*. Cambridge: Cambridge University Press.
4. W. D. IWAN 1967 *Transactions of the American Society of Mechanical Engineers*, *Journal of Applied Mechanics* (September), 612–617. On a class of models for the yielding behavior of continuous and composite systems.

APPENDIX: NOMENCLATURE

a_{ij}	dynamic stiffness coefficients	n	index
c_i	internal viscous damping coefficient	n_{sup}	number of cycles with super-frequency
c_{eq}	equivalent viscous damping coefficient	r	material parameter
$c_{(\omega-\Omega)}$, $c_{(\omega+\Omega)}$	equivalent viscous damping coefficients	t	time
E_i	elastic modulus	x, y, z	Cartesian co-ordinates
E_t	elastic modulus	x_e, y_e	Cartesian co-ordinates in the bearings
F	load	x_0, y_0, x_{e0}, y_{e0}	amplitudes
f_e	natural frequency	α	phase angle
$f_1(\varepsilon), f_2(\varepsilon)$	functions of strain	ΔU	dissipation energy
H	material parameter	ε	strain
h_i	internal hysteretic damping coefficient	ε_a	strain amplitude
		ξ–η–z	rotating co-ordinate system
i	$=\sqrt{-1}$	η	loss coefficient
k_i	stiffness coefficient	σ	normal stress
$k_{xx,\ldots}$	journal bearing stiffness coefficient	$\sigma_{f,i}$	normal stress
		σ_a	normal stress amplitude
L	length	Ω	angular rotational frequency of the shaft
m	mass	ω	angular frequency